Supplementary Information

Triplex metallohelices have enantiomer-dependent mechanisms of action in colon cancer cells

J. P. C. Coverdale,[a,b] H. Kostrhunova,[c] L. Markova,[c] H. Song,[a,d] M. Postings,[a] H. E. Bridgewater,[a,e] V. Brabec*,[c] N. J. Rogers*,[a] P. Scott*[a]

[a.] *Department of Chemistry, University of Warwick, Coventry, CV4 7AL, UK.*
[b.] *School of Pharmacy, Institute of Clinical Sciences, University of Birmingham, Edgbaston, B15 2TT, UK*
[c.] *The Czech Academy of Sciences, Institute of Biophysics, Kralovopolska 135, CZ-61265 Brno, Czech Republic*
[d.] *Beijing Area Major Laboratory of Peptide and Small Molecular Drugs, School of Pharmaceutical Sciences, Capital Medical University, Beijing, 100069, China*
[e.] *Centre of Exercise, Sport and Life Science, Faculty of Health and Life Sciences, Coventry University, Coventry, CV1 5FB, UK*

Table of Contents

1. Synthesis and Characterisation

1.1 Solvents and chemicals

All solvents and chemicals purchased from commercial sources (Sigma-Aldrich, Acros, Fisher Scientific, Alfa Aesar or Invitrogen) were used without further purification unless otherwise stated.

1.2 Characterisation of compound Λ-1'

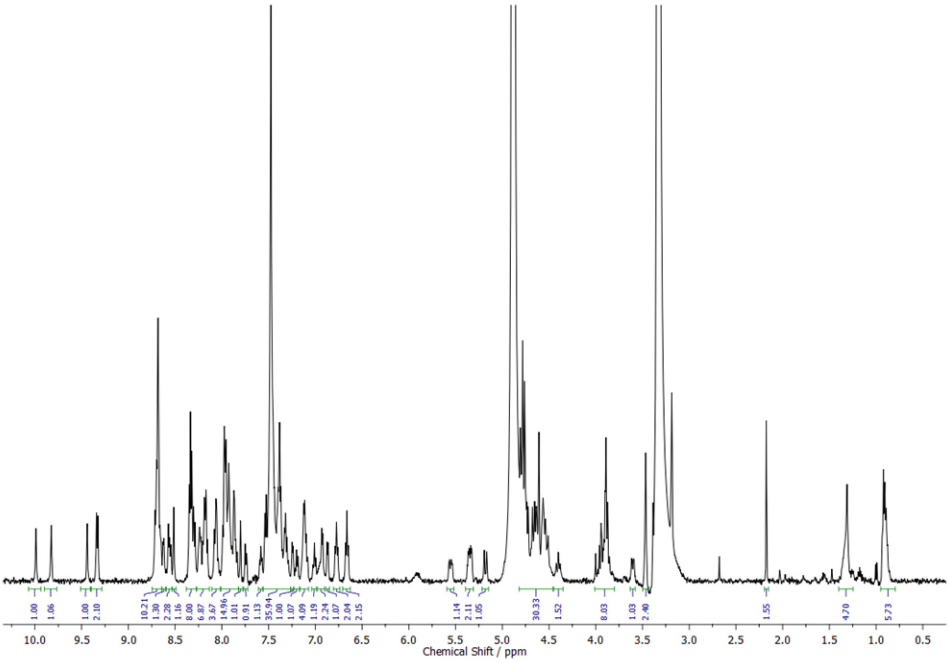

Figure S1 ^{1}H NMR (500 Mz, CD_3OD, 298 K) of **Λ-1'**.

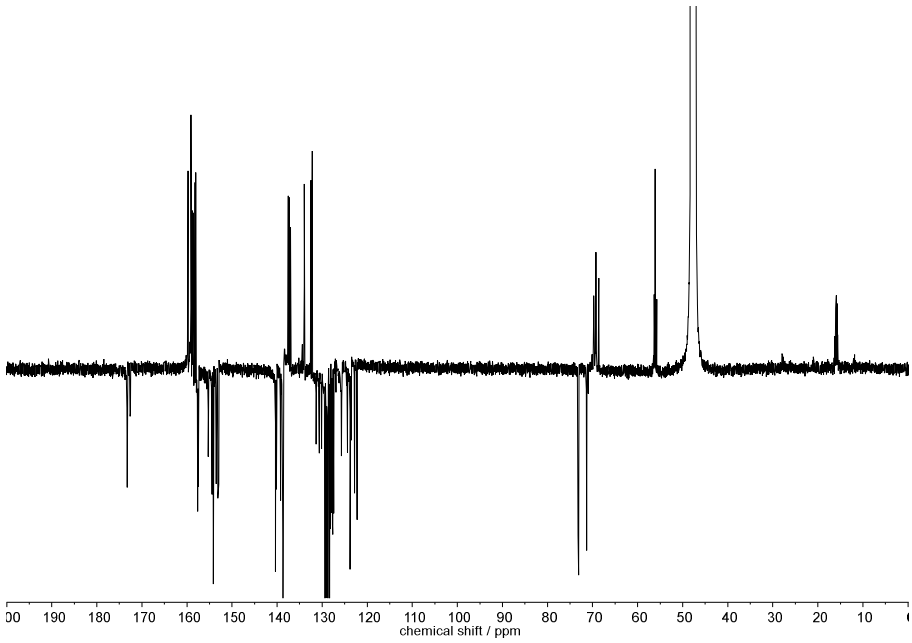

Figure S2 ^{13}C NMR (125 Mz, CD_3OD, 298 K) of **Λ-1'**.

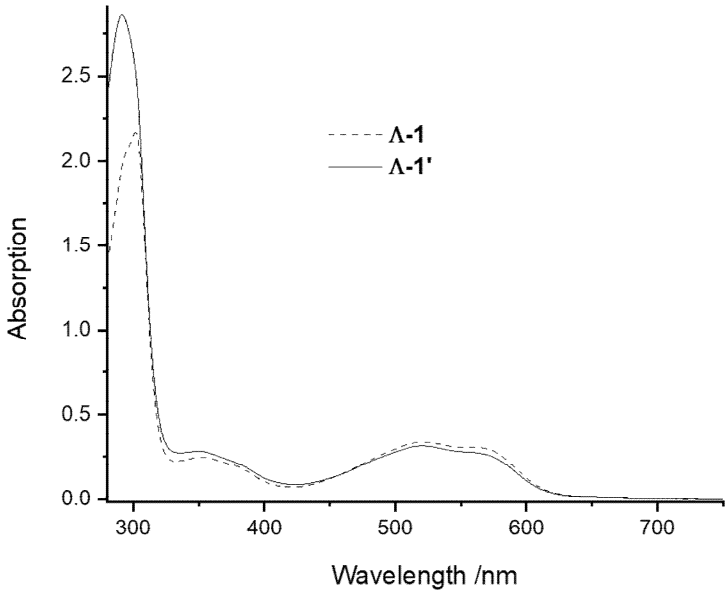

Figure S3. UV-Vis absorption spectra of **Λ-1** (dashed) and **Λ-1'** (solid), 20 μM methanol solution.

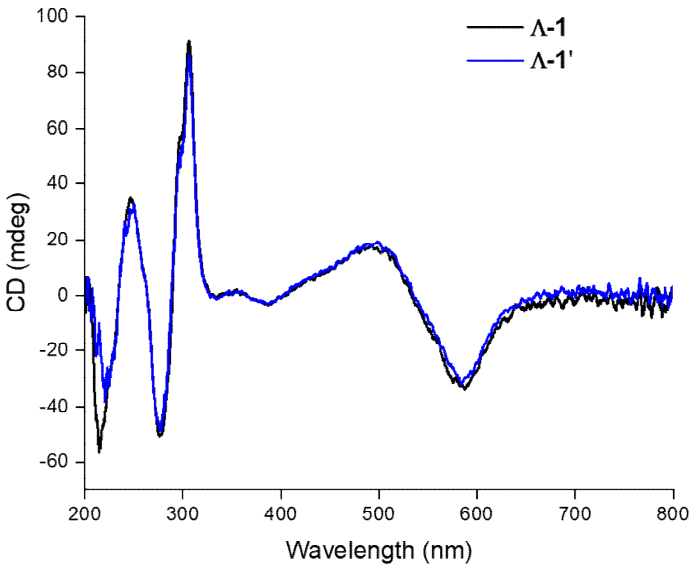

Figure S4. Circular dichroism spectra of **Λ-1**(black) and **Λ-1'** (blue), 20 μM methanol solution.

HRMS Calculated for $[L+Na]^+$ m/z 417.1686, found m/z 417.1688; $[^{57}Fe_2L_3]^{4+}$ m/z 324.1017, found m/z 324.1016; $[^{57}Fe_2L_3]Cl^{3+}$ m/z 443.7920, found m/z 443.7921; $[^{57}Fe_2L_3]Cl_2^{2+}$ m/z 683.1727, found m/z 683.1721; FT-IR cm^{-1} 3346 br, 3028 w, 1631

m, 1603 m, 1493 m, 1467 m, 1440 m, 1404 w, 1360 w, 1319 w, 1294 s, 1241 m, 1160 w, 1103 m, 1074 s, 1008 w, 936 m, 836 w, 755 m.

2. Antiproliferative activities and metallohelix accumulation in HCT116 cells

2.1 Time-dependent antiproliferative activities

Table S1. Time-dependence of antiproliferative activities (IC_{50} / μM) for enantiomeric Fe complexes **Λ-1** and **Δ-1** in HCT116 human colorectal carcinoma cells. Measured using SRB Assay.

	IC_{50} (μM)					
	3 h	6 h	12 h	24 h	48 h	96 h
Λ-1	73 ± 1	71 ± 2	56 ± 2	30.6 ± 0.5	4.2 ± 0.1	3.4 ± 0.7
Δ-1	68 ± 1	63 ± 1	53 ± 1	38 ± 2	14 ± 1	11.5 ± 0.7

2.2 Temperature-dependent antiproliferative activities

Table S2. Temperature-dependence of intracellular iron accumulation (ng ^{57}Fe × 10^6 cells) for enantiomeric Fe complexes **Λ-1'** and **Δ-1'** in HCT116 human colorectal carcinoma cells, treated in an equimolar manner (3 μM).

	Λ-1'	Λ-1'	Δ-1'	Δ-1'
Time / h	277 K	310 K	277 K	310 K
3	18 ± 2	27.9 ± 0.5	17 ± 2	23 ± 1
6	22 ± 5	32 ± 1	22 ± 4	27 ± 2

2.3 Time-dependent cellular accumulation of metallohelices

Table S3. Time-dependence of intracellular iron accumulation (ng $^{57}Fe \times 10^6$ cells) for enantiomeric Fe complexes **Λ-1'** and **Δ-1'** in HCT116 human colorectal carcinoma cells, treated in an equimolar manner (3 μM).

	Intracellular iron accumulation (ng $^{57}Fe \times 10^6$ cells)	
	Λ-1'	Δ-1'
Time / h		
0	0.31 ± 0.04	0.31 ± 0.04
1	19 ± 1	14.3 ± 0.7
3	27.9 ± 0.5	23 ± 1
6	32 ± 1	27 ± 2
18	57.6 ± 0.3	54 ± 9
24	68 ± 3	65 ± 2
48	48 ± 4	53 ± 3
72	33 ± 4	49 ± 4
96	26 ± 2	43 ± 3

2.4 Time-dependent and recovery-dependent antiproliferative activities

Table S4. Time-dependence and recovery-dependence of antiproliferative activities (IC_{50} / μM) for enantiomeric Fe complexes **Λ-1** and **Δ-1** in HCT116 human colorectal carcinoma cells. Cells were either treated for 24 h + 72 h recovery time in metal complex-free medium (24 / 72), or treated for 96 h without recovery time (96 / 0) for a total of 3-96 h.

		IC_{50} (μM)					
	Exposure / Recovery (h)	3 h	6 h	12 h	24 h	48 h	96 h
Λ-1	24 / 72	[73 ± 1]	[71 ± 2]	[56 ± 2]	[30.6 ± 0.5]	5.1 ± 0.1	7.1 ± 0.2
Λ-1	96 / 0	73 ± 1	71 ± 2	56 ± 2	30.6 ± 0.5	4.2 ± 0.1	3.4 ± 0.7
Δ-1	24 / 72	[68 ± 1]	[63 ± 1]	[53 ± 1]	[38 ± 2]	39 ± 4	51.9 ± 0.8
Δ-1	96 / 0	68 ± 1	63 ± 1	53 ± 1	38 ± 2	14 ± 1	11.5 ± 0.7

2.5 Time-dependent and recovery-dependent cellular accumulation of metallohelices

Table S5. Time-dependence and recovery-dependence of intracellular iron accumulation (ng $^{57}Fe \times 10^6$ cells) for enantiomeric Fe complexes **Λ-1'** and **Δ-1'** in HCT116 human colorectal carcinoma cells, treated in an equimolar manner (3 μM). Cells were either exposed to Fe complexes for 0-96 h without recovery time (96 / 0) or exposed for 24 h + 72 h recovery time in metal complex-free medium (24 / 72) for a total of 0-96 h.

	Intracellular iron accumulation (ng $^{57}Fe \times 10^6$ cells)			
	Λ-1'	Λ-1'	Δ-1'	Δ-1'
Total time / h	96 / 0	24 / 72	96 / 0	24 / 72
0	0.31 ± 0.04	0.31 ± 0.04	0.31 ± 0.04	0.31 ± 0.04
1	19 ± 1	19 ± 1	14.3 ± 0.7	14.3 ± 0.7
3	27.9 ± 0.5	27.9 ± 0.5	23 ± 1	23 ± 1
6	32 ± 1	32 ± 1	27 ± 2	27 ± 2
18	57.6 ± 0.3	57.6 ± 0.3	54 ± 9	54 ± 9
24	68 ± 3	68 ± 3	65 ± 2	65 ± 2
48	48 ± 4	42.7 ± 0.8	53 ± 3	41 ± 3
72	33 ± 4	33 ± 4	49 ± 4	32 ± 4
96	26 ± 2	20 ± 4	43 ± 3	24 ± 3

2.6 Cellular distribution of metallohelices

Table S6. Cellular ^{57}Fe distribution in HCT116 colorectal cancer cells treated with equimolar concentrations (3 μM) of enantiomeric Fe complexes **Λ-1'** or **Δ-1'**. Cells were fractioned using the FractionPREP™ Cell Fractionation Kit (Biovision). Four fractions are obtained: (i) cytosolic fraction, (ii) membrane fraction, (iii) nucleic fraction, and (iv) cytoskeletal fraction. Fractions were analysed for ^{57}Fe content by ICP-MS.

	Cellular ^{57}Fe fractionation (%)			
	Cytosolic	Membrane	Nucleic	Cytoskeletal
Λ-1' (24 h)	0.25 ± 0.05	3.3 ± 0.2	2.8 ± 0.9	94 ± 5
Λ-1' (96 h)	0.5 ± 0.1	8.4 ± 0.2	4.1 ± 0.4	87 ± 4
Δ-1' (24 h)	0.26 ± 0.05	3.4 ± 0.2	3.3 ± 0.6	93 ± 5
Δ-1' (96 h)	0.2 ± 0.1	7 ± 1	4.1 ± 0.3	88 ± 2

3. Interaction of metallohelices with biomolecules in vitro

3.1 Tubulin binding

Tubulin from porcine brains was incubated at 15 μM in BRB80 buffer, in the presence of GMPCPP (1 mM) at 37 ºC for 1 h with Λ-1 or Δ-1 (50 μM). The samples were spun down in an ultracentrifuge (25 psi, 10 min), the supernatant was recovered and the pellet was incubated in ice for 10 min with ice-cold BRB80 buffer (65 μL), and subsequently resuspended and stored on ice. The concentration of metallohelix in each resuspended pellet / supernatant sample was measured using UV-Vis absorption spectroscopy, whist the protein. All samples were measured in triplicate.

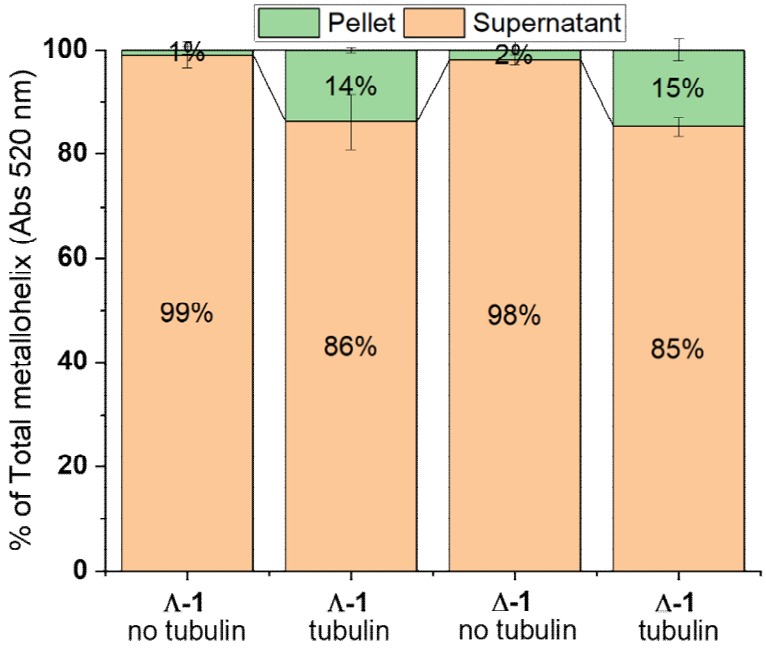

Figure S5. Interaction of metallohelices with tubulin protein. % of total metallohelix concentration detected in the pellet of supernatant of sample (determined by measuring the UV-Vis absorption at 520 nm) following incubation of tubulin (15 μM) in BRB80 buffer with **Λ–1** or **Δ-1** (50 μM) in the presence of GMPCPP (1 mM) for 1 h, at 37 ºC. Control samples were also tested without tubulin. The samples were spun down at 25 psi for 10 min, to separate polymerised microtubules from free tubulin in solution, and the pellet was resuspended in buffer

3.2 Ct-DNA Binding by fluorescence competition assays

A solution (10 mM Tris buffer, pH 7.4, 1 mM EDTA) of 3.9 μM ct-DNA with 1.3 μM ethidium bromide/Hoechst 33258/methyl green was titrated by an aliquots of stock (100 μM) metallohelix. The DNA-EtBr complexes were excited at 520 nm and fluorescence intensity was measured at 550-700 nm after each titration of metal complex, the DNA-Hoechst complexes were excited at 345 nm and the fluorescence intensity was measured at 360-600

nm, and the DNA-methyl green complexes were excited at 640 nm and the fluorescence intensity was measured at 650- 750 nm The standard parameters used were: response time 1 sec, data pitch 1 nm, scanning speed 100 nm/min and accumulation 1.

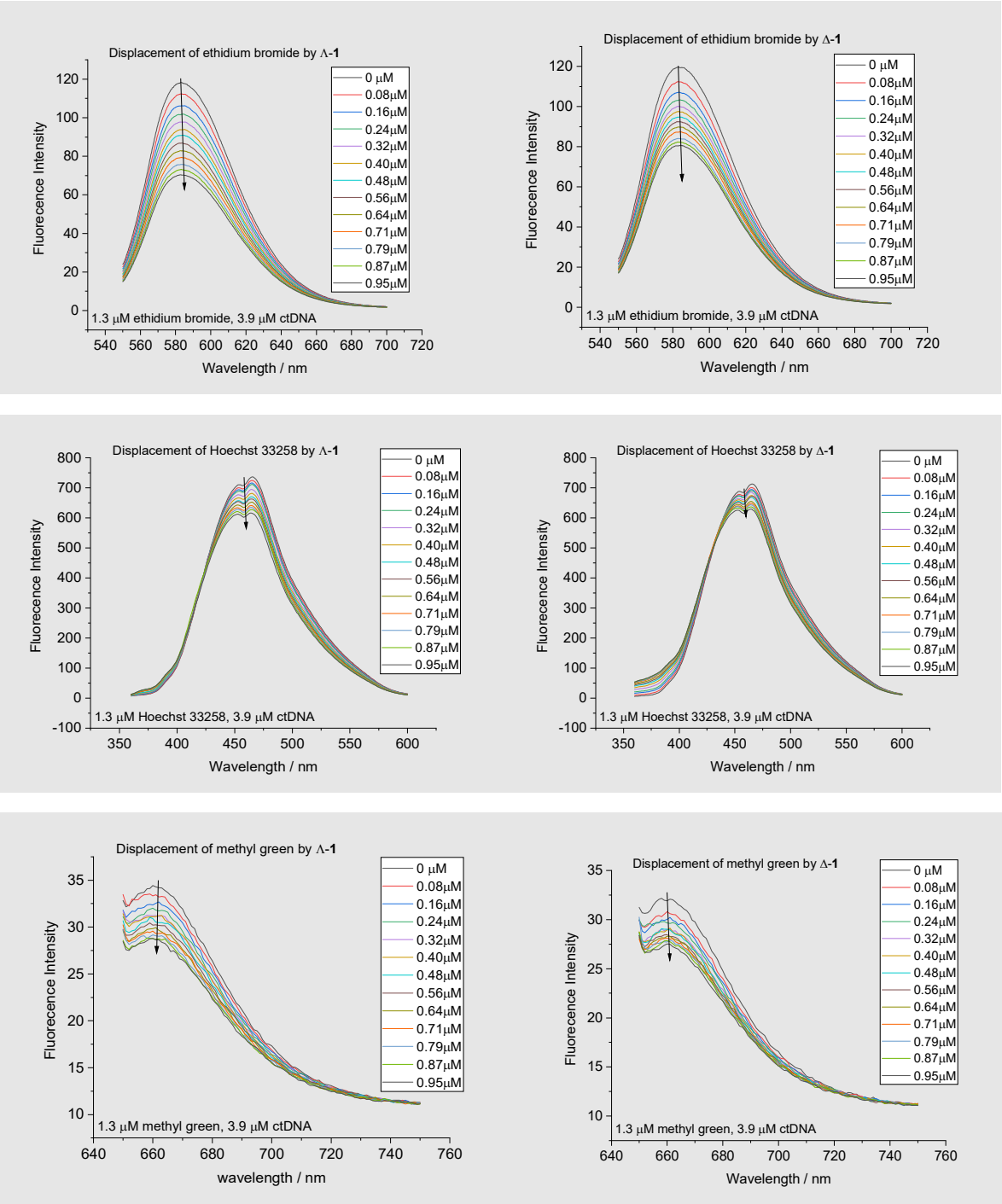

Figure S6. Fluorescence competition assays – raw data: The ct-DNA (3.9 μM) was firstly incubated with fluorescent binder (1.3 μM) in Tris biffer (pH 7.4), then titrated with variable concentration of metallohelices (0-0.95 μM), and the fluorescence was measured.

We observed the displacement of the fluorescent intercalator ethidium bromide, the minor groove binder Hoechst 33258 and major groove binder methyl green by both **Λ-1** and **Δ-1**.

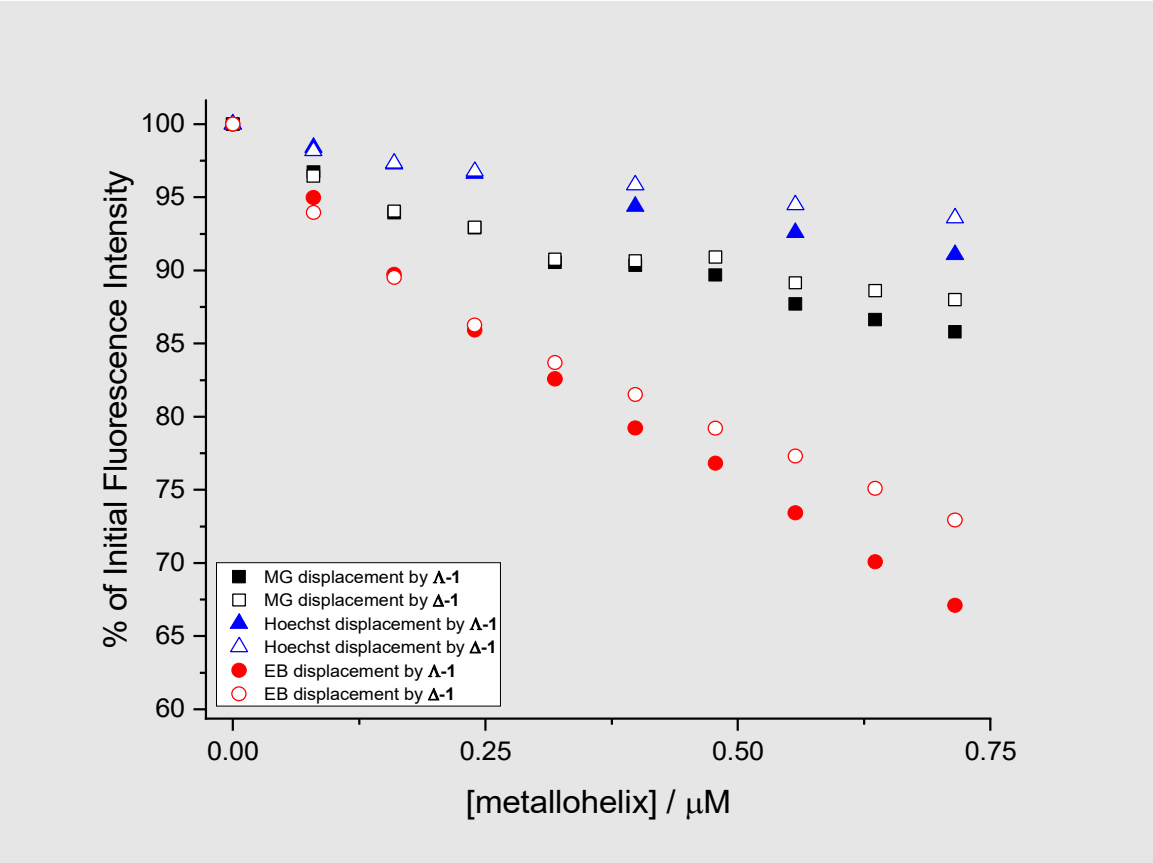

Figure S7. Fluorescence competition assay: The ct-DNA (3.9 μM) was firstly incubated with fluorescent binder (1.3 μM) in Tris biffer (pH 7.4), then titrated with variable concentration of metallohelices (0-0.75 μM). The % of initial fluorescence intensity with the addition of complex versus concentration of metallohelices is plotted. Ethidium bromide (DNA intercalator binder), fluorescence signal measured at 583 nm = red symbols; hoechst (DNA minor grove binder), fluorescence signal measured at 465 nm = blue symbols; methyl green (DNA major grove binder), fluorescence signal measured at 661 nm = black symbols.